Targeting of Moloney Murine Leukemia Virus Gag Precursor to the Site of Virus Budding

Maarit Suomalainen, Kjell Hultenby,* and Henrik Garoff

Department of Bioscience at Novum, and *Clinical Research Center, Karolinska Institutet, Novum, Sweden

Abstract. Retrovirus Moloney murine leukemia virus (M-MuLV) matures by budding at the cell surface. Central to the budding process is the myristoylated viral core protein precursor Gag which, even in the absence of all other viral components, is capable of associating with the cytoplasmic leaflet of the plasma membrane and assembling into extracellular virus-like particles. In this paper we have used heterologous, Semliki Forest virus-driven, expression of M-MuLV Gag to study the mechanism by which this protein is targeted to the cell surface. In pulse-chase experiments, BFA, monensin, and 20°C block did not affect incorporation of Gag into extracellular particles thereby indicating that the secretory pathway is not involved in targeting of Gag to the cell surface. Subcellular fractionation studies demonstrated that newly synthesized Gag became rapidly and efficiently associated with membranes which had a density similar to that of plasma membrane–derived vesicles. Protease-protection studies confirmed that the Gag-containing membranes were of plasma membrane origin, since in crude cell homogenates, the bulk of newly synthesized Gag was protease-resistant as expected of a protein that binds to the cytoplasmic leaflet of the plasma membrane. Taken together these data indicate that targeting of M-MuLV Gag to the cell surface proceeds via direct insertion of the protein to the cytoplasmic side of the plasma membrane. Furthermore, since the membrane insertion reaction is highly efficient and specific, this suggests that the reaction is dependent on as-yet-unidentified cellular factors.

The last step in the assembly of enveloped viruses is budding of the genome-containing viral core structure through a specific membrane compartment. During this process the core is wrapped into a membrane that is highly enriched in virally encoded spike proteins. Studies on genetically altered viruses have indicated that viral budding reactions can proceed by three different kinds of interactions. In the case of alphaviruses, production of enveloped particles is strictly dependent on coexpression of the core and spike proteins (33, 54), thereby indicating that the budding reaction is driven by interactions between the cytoplasmic core and transmembrane spike proteins. The envelopment of hepadnavirus core has also been shown to require viral spike proteins (5), but since hepadnaviral spike proteins are capable of self-assembling into subviral lipoprotein particles (50), lateral spike–spike interactions alone in this case are evidently sufficient to induce an extrusion of a membrane vesicle. Also, the spike proteins of flaviviruses (2, 24, 34, 63) and coronaviruses (58) have been demonstrated to form subviral lipoprotein particles. Retroviruses represent yet a third type of viral budding mechanism, and in this case the viral core protein precursor Gag is capable of self-assembling into enveloped virus-like particles (9, 12, 48, 53, 62), thereby indicating that binding of a cytoplasmic core protein into the membrane and its oligomerization into a core structure provide the driving force for retrovirus budding. Recently, it was reported that the core components of the rhabdovirus rabies virus was capable of assembling into extracellular enveloped particles in the absence of the viral spike proteins (36).

One characteristic feature of viral budding reactions is their localization to specific cellular compartments. The prevailing view has been that the site of virus budding is determined by intracellular localization of viral spike proteins (reviewed in reference 46). This view assumes that cytoplasmic core components are devoid of targeting signals and are recruited into the budding compartment via interaction with the cytoplasmic tails of the spike proteins. This model most likely holds true for viruses like alphaviruses and hepadnaviruses, where the core lacks membrane binding activity and is dependent on spike proteins for its envelopment (5, 33, 54, 65). However, the model cannot apply to retroviruses. Budding of retroviruses occurs at the

Please address all correspondence to H. Garoff, Department of Bioscience at Novum, S-141 57 Huddinge, Sweden. Tel.: 46 8 608 9125. Fax: 46 8 774 5538.

The current address of M. Suomalainen is University of Zurich, Department of Zoology,/Section Cell Biology, Winterthurerstr. 190, CH-8057 Zurich, Switzerland.

cell surface and since the core protein precursor Gag efficiently assembles into extracellular particles when expressed alone (9, 12, 48, 53, 62), it is evident that targeting of Gag to the cell surface is independent of viral spike proteins. How this targeting is achieved is at present unknown.

Most retroviral Gag precursors are myristoylated proteins and are expected to be synthesized on free ribosomes in the cytoplasm like other myristoylated proteins (21). In the case of type C retroviruses (e.g., Moloney murine leukemia virus [M-MuLV][1]) and lentiviruses (e.g., Human immunodeficiency virus type 1 [HIV-1]), viral core structures are formed at the plasma membrane, concomitantly with the budding process, and therefore Gag precursors of these viruses are presumed to be targeted to the cell surface as monomers or as homo-oligomers of smaller than full-sized cores (61). The NH_2-terminal myristate modification has been demonstrated to be essential for the membrane association and budding competence of these Gag precursors (6, 9, 12, 47). Efficient binding of HIV-1 Gag to membranes has been shown to require also a cluster of basic amino acids located at the amino-terminal part of the protein (64, 66). These basic amino acids most likely strengthen the membrane association of HIV-1 Gag by interacting with acidic membrane phospholipids (35, 66). Similar highly basic domains are found in the amino-termini of Gag precursors of other retroviruses as well (66), and so presumably in these cases, the membrane association is also mediated by both hydrophobic and electrostatic interactions. However, since neither myristoylated proteins nor acidic phospholipids are restricted to the plasma membrane (39, 56, 57), the targeting of Gag to the cell surface poses a puzzle. One possibility is that targeting is actually achieved by quite unspecific means; Gag precursors could be initially randomly inserted into all membranes, and then routed from the endoplasmic reticulum (ER) and Golgi to the plasma membrane via the secretory pathway. Another possibility is that the membrane insertion reaction is restricted to the plasma membrane, perhaps due to the interaction of Gag precursors with a specific plasma membrane-associated Gag "receptor" (or receptors). Previous studies using inhibitors of the secretory pathway to distinguish between these two possibilities have yielded conflicting results: the carboxylic ionophore monensin, which blocks the secretory pathway at the level of Golgi (16, 55), has been reported to decrease the release of M-MuLV particles from infected cells (18), whereas in the case of HIV-1, monensin was found to have no effect on the assembly of Gag into extracellular particles (42). Furthermore, the assembly of both HIV-1 and M-MuLV Gag precursors into extracellular particles has been reported to be insensitive to brefeldin A (BFA) (26, 43), a fungal antibiotic that blocks exit of proteins from the ER (23). Due to these conflicting results, the pathway by which retroviral Gag precursors are targeted to the cell surface has remained unresolved.

In this work we have studied intracellular targeting of M-MuLV Gag by using recombinant Semliki Forest virus (SFV) genomes to express high levels of M-MuLV Gag in cells. This enabled us to quantitatively assay the membrane insertion of a newly synthesized Gag precursor. Our results show that the M-MuLV Gag is directly inserted into the plasma membrane without first becoming associated with ER or Golgi membranes. Furthermore, the insertion of M-MuLV Gag to the plasma membrane was found to occur rapidly after the synthesis of the protein, with high efficiency and specificity. Since the presumed membrane anchor of Gag precursors is not expected to confer specific insertion into the plasma membrane, our results suggest that the membrane insertion of Gag is dependent on as-yet-unidentified cellular components.

1. *Abbreviations used in this paper*: HIV-1 Human immunodeficiency virus type 1; M-MuLV, Moloney murine leukemia virus; PNS, post-nuclear supernatant; SFV, Semliki Forest virus; TR, transferrin receptor.

Materials and Methods

Cells and Virus

BHK-21 cells (obtained from American Type Culture Collection, Rockville, MD) were grown in BHK-21 medium supplemented with 5% FCS, 20 mM Hepes (*N*-2-hydroxyethylpiperazine-N'-2-ethanesulfonic acid, pH 7.3), 10% tryptose phosphate broth, and 2 mM glutamine (all cell culture media were from GIBCO BRL, Gaithersburg, MD). Infectious SFV particles expressing the Gag precursor of M-MuLV were prepared by coelectroporating equal amounts (20 μl) of in vitro transcribed SFV-C/Pr65gag (53) and helper 1 (30) RNAs into 10^7 BHK-21 cells as described in Suomalainen and Garoff (53). At 20–22 h postelectroporation, culture media containing infectious virus were collected and the cell debris was removed by centrifugation at 800 *g* for 15 min at +4°C. The clarified culture medium was used for infections without further concentration. The titer of the virus stock was determined by indirect immunofluorescence using polyclonal rabbit anti-p30 antiserum (a generous gift from Dr. G. Schmidt, Institut für Molekulare Virologie, GSF, Munich, Germany). Infectious recombinant SFV particles expressing the TRΔ2 mutant of human transferrin receptor were prepared similarly by using SFV-C/TRΔ2 (53) and helper 1 RNAs, and titer of the virus stock was determined by indirect immunofluorescence using a monoclonal anti-human transferrin receptor antibody (ascites fluid of OKT-9, preparation was provided by Dr. T. Ebel at the laboratory). Wild-type SFV stocks were prepared in BHK-21 cells as previously described (22).

Analysis of Release of Gag Particles from Cells

BHK-21 cells grown on 35-mm-diam dishes (duplicate plates) were infected with recombinant SFV-C/Pr65gag particles diluted in minimum essential medium (MEM) supplemented with 0.2% bovine serum albumin, 10 mM Hepes, and 2 mM glutamine at a multiplicity of infection of ~5–10. After 60 min at 37°C, the virus inoculum was removed and cells were further incubated at 37°C in the same medium. At 4 h postinfection, intracellular methionine was depleted by incubating cells in a methionine-free MEM supplemented with 10 mM Hepes and 2 mM glutamine for 30 min at 37°C. After this starvation, the medium was replaced with the same methionine-free medium containing 100 μCi of [^{35}S]methionine (Amersham) per ml, and the cells were incubated at 37°C for 5 min or 10 min (pulse). After the pulse, cells were washed once with chase medium (minimum essential medium supplemented with 10 mM Hepes and 2 mM glutamine and containing 100-fold excess of cold methionine) and then incubated in the same medium for 5 min to 2 h (chase). After the chase, culture media were collected and clarified by centrifugation in an Eppendorf centrifuge (5 min at 5,000 rpm at 4°C). Gag particles were harvested from clarified culture media by pelleting them through a 20% sucrose cushion in a Vti75 rotor at 35,000 rpm for 1 h at 4°C using adaptors for Eppendorf tubes (Beckman Instrs., Fullerton, CA). Pelleted particles were taken up into SDS-sample buffer and analyzed by SDS-PAGE as described (53). Cell monolayers were washed with PBS (without $MgCl_2$ and $CaCl_2$) and solubilized with 1% SDS containing 10 mM iodoacetamide (45). Aliquots of cell lysates were mixed with SDS-sample buffer and analyzed by SDS-PAGE. Radioactivity in protein bands was determined by using a Bas-III Image Plate and the Bio-Image analyzer system Bas 2000 (Fuji Photo film Co.). The effect of BFA on release of Gag particles was tested by including 10 μg/ml of BFA (Boehringer Mannheim Corp., Indianapolis, IN, BFA stock prepared in ethanol [EtOH]:H_2O [1:1]) into methionine-star-

vation medium, pulse, and chase media. An equivalent volume of EtOH: H_2O was added to the mock-treated cells. The effect of monensin on the release of Gag particles was tested by including 5 μM monensin (Sigma, stock prepared in EtOH) into starvation, pulse and chase media, and an equivalent volume of EtOH was added to the mock-treated cells. To test the effect of 20°C block on the release of Gag particles, starvation, pulse, and chase were done as above except that plates were incubated in a 20°C water bath and media devoid of $NaHCO_3$ was used throughout. Control cells were shifted to a 37°C water bath after the pulse.

Analysis of Transport of SFV Spike Complex to the Cell Surface

BHK-21 cells grown on 35-mm-diam dishes (duplicate plates) were infected with SFV at a multiplicity of infection of 10 as described above for recombinant SFV infections. At 4 h postinfection, intracellular methionine was depleted by incubating cells in a methionine-free MEM for 30 min, after which cells were metabolically labeled with [^{35}S]methionine for 10 min and chased for 5/90/180 min as described above. After the chase, plates were placed on ice and proteins at the plasma membrane were labeled with NHS-SS-biotin (Pierce, Rockford, IL) at 4°C as described (31). Biotinylated proteins were precipitated from cell lysates using streptavidin-agarose (Sigma) as described (19). Precipitates were taken up into SDS-sample buffer and analyzed by SDS-PAGE together with aliquots of total cell lysates. Radioactivity in protein bands was quantitated as described above. The effects of BFA and monensin treatments on the transport of the spike complex to the cell surface was analyzed as described above for SFV-C/Pr65gag–infected cells. The analysis of the affect of 20°C block was done as described for SFV-C/Pr65gag–infected cells except that starvation and pulse were at 37°C and cells were shifted to 20°C only for the chase.

Analysis of Kinetics and Efficiency of Membrane Association of M-MuLV Gag

BHK-21 cells grown on 55-mm-diam dishes were infected with the recombinant SFV-C/Pr65gag virus as described above. At 4 h postinfection intracellular methionine was depleted from cells by a 30-min incubation in methionine-free MEM, after which cells were metabolically labeled with [^{35}S]methionine for 5 min and chased for 0/5/15/30 min. After the chase, plates were placed on ice, washed twice with ice-cold PBS after which cells were scraped into PBS and harvested by centrifugation in an Eppendorf centrifuge (5 min at 2,000 rpm at 4°C). The cell pellet was taken up into homogenization buffer (10 mM Tris-HCl, pH 7.4, 0.25 M sucrose, 20 μg/ml PMSF [Sigma Chem. Co., St Louis, MO]) and cells were disrupted by pulling the cell suspension through a 23-G (0.6 mm × 25 mm) needle fifteen times. Nuclei and debris were removed by centrifugation at 5,000 rpm for 5 min at 4°C to yield postnuclear supernatant (PNS) fraction. Typically 65–70% of total Gag was recovered in the PNS fraction. 2 ml 70% (wt/wt) sucrose was mixed with 0.5 ml PNS fraction, placed at the bottom of an SW50.1 centrifuge tube (Beckman Instrs.), and overlaid with 2 ml 65% (wt/vol) and 0.5 ml 10% (wt/vol) sucrose. The step gradient was then centrifuged to an equilibrium at 35,000 rpm for 18 h at 4°C. Fractions (1 ml) were collected from the top and aliquots of fractions were mixed with SDS-sample buffer and analyzed by SDS-PAGE. Radioactivity in protein bands was quantitated as described above.

Subcellular Fractionation

BHK-21 cells grown on 55-mm-diam dishes were infected with the recombinant SFV-C/Pr65gag virus, labeled with [^{35}S]methionine for 10 min at 4.5 h postinfection and chased for 0/10/30/60 min after which cell homogenates were prepared as described above. For the ATP depletion experiment, cells were placed on ice after pulse and incubated for 10 min in a glucose-free medium containing 10 mM sodium azide, 20 mM 2-deoxy-D-glucose, and an excess of unlabeled methionine (3, 25). Subsequently, cells were incubated at 37°C in the same medium for 30 min before homogenization. A modification of the step gradient described by Saraste et al. (49) was used for fractionation of the PNS. Briefly, 0.5 ml PNS was mixed with 3 ml 65% sucrose, placed at the bottom of an SW41 centrifuge tube and overlaid with 1 ml 53%, 2 ml each of 40%, 35% and 30%, and 1.5 ml of 10% sucrose (all sucrose solutions were wt/wt; Beckman Instrs.). The gradient was then centrifuged to equilibrium at 37,000 rpm for 14 h at 4°C. Fractions (1 ml) were collected from the top, and aliquots of fractions were TCA-precipitated by adding equal volume of 20% TCA. The TCA-precipitated proteins were taken up into SDS-sample buffer, analyzed by SDS-PAGE and radioactivity in protein bands was quantitated as described above. To determine the position of ER in the gradient, PNS fractions prepared from SFV-C/TRΔ2–infected cells that had been pulse-labeled for 10 min and chased for 5 min were analyzed on the gradient and the radioactively labeled TRΔ2 was used as a marker for ER. The position of plasma membrane in the gradient was determined by analyzing PNS prepared from SFV-C/TRΔ2–infected cells that had been pulse-labeled for 20 min and chased for 3 h, and the slower migrating form of TRΔ2 (38, 53) was used as a marker for the plasma membrane. Galactosyl transferase activity, a marker for *trans*-Golgi, was assayed in the gradient fractions as described in Brew et al. (4).

Protease Protection Assay

BHK-21 cells grown on 55-mm dishes were infected with SFV-C/Pr65gag, and at 4.5 h postinfection cells were metabolically labeled with [^{35}S]methionine (100 μCi/1 ml) for 10 min and chased for 2 min. Cells were homogenized in 800 μl homogenization buffer and 100 μl aliquots of PNS-fractions were treated with 8 μg/ml proteinase K (Boehringer Mannheim) for 30 min at 0°C in the presence and absence of 1% NP-40. Digestion was stopped by adding PMSF to a final concentration of 0.4 mg/ml and samples were further incubated at 0°C for 10 min after which time proteins were TCA-precipitated by adding 100 μl of 20% TCA. Precipitates were taken up into SDS-sample buffer and analyzed by SDS-PAGE. In mock-treated samples, protease was omitted and in one control sample the PMSF was present from the beginning.

Electron Microscopy

For the analysis of plasma membrane vs Golgi budding, SFV-C/Pr65gag–infected cells were fixed at 6 h post infection with 2% glutaraldehyde in 0.1 M sodiumcacodylate buffer (pH 7.4) for 24 h. Cells were scraped off with a wooden pin and pelleted at 500 *g*. After washing in 0.1 M sodiumcacodylate buffer, cells were postfixed in 2% osmium tetroxid in 0.1 M sodiumcacodylate buffer (pH 7.4) at 4°C for 2 h and dehydrated for 15 min in 70%, 95%, and 100% ethanol at 4°C. 2% uranyl acetate was added to the final ethanol step. After dehydration the cells were placed in pure acetone for 15 min and embedded in LX-112 (Ladd, Vermont) and polymerized at 60°C. Ultrathin sections were contrasted with uranyl acetate and lead citrate and analyzed in a Philips 420 electron microscope at 80 kV.

Results

Expression of M-MuLV Gag from Recombinant SFV Genomes

Intracellular targeting of M-MuLV Gag-precursor (Pr65^{gag}) is difficult to study using wild-type M-MuLV–infected cells due to the low level of expression of viral proteins in these cells. Therefore a heterologous, SFV-driven expression system was chosen for the expression of Pr65^{gag} (30, 51). We have previously described the construction of a recombinant SFV genome SFV-C/Pr65gag, in which the coding sequence of Pr65^{gag} is fused to the C-gene of SFV (53). This SFV-C/Pr65^{gag}-genome directs a high level of synthesis of a C-Pr65^{gag}-fusion protein, which is cotranslationally processed into C and Pr65^{gag} proteins by the autoproteolytic activity of the SFV C protein (1, 37). In our previous study we also showed that Pr65^{gag} expressed from the SFV-C/Pr65gag-genome becomes myristoylated and assembles into extracellular virus-like particles which are similar to immature M-MuLV virions (53). A more detailed analysis of the kinetics and efficiency of release of Gag particles from SFV-C/Pr65gag–infected BHK-21 cells is presented in Fig. 1. At 4.5 h postinfection cells were metabolically labeled with [^{35}S]methionine for 5 min and chased for 0 min–2 h, and the amount of Pr65^{gag} in cell lysates and extracellular particles was determined. Aliquots

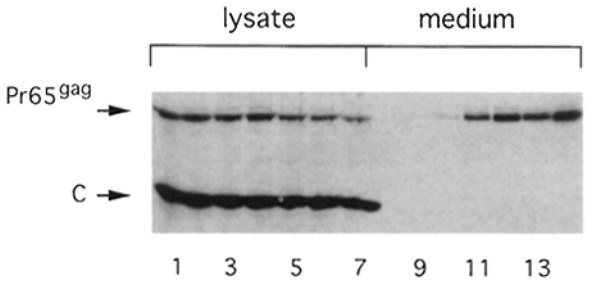

Figure 1. Kinetics and efficiency of release of Gag particles from SFV-C/Pr65gag–infected cells. SFV-C/Pr65gag–infected cells were metabolically labeled with [^{35}S]methionine for 5 min and chased for 0 min–2 h, and the amount of Pr65^{gag} in cell lysates (lanes *1–7*) and extracellular particles (medium; lanes *8–14*) was analyzed by SDS-PAGE and fluorography. Aliquots of cell lysates were directly analyzed by SDS-PAGE, whereas extracellular particles were first concentrated by pelletation through a sucrose cushion. Proportionally five times more of medium samples than lysate samples were loaded on the gel. Lanes *1* and *8*, 0-min chase; lanes *2* and *9*, 5-min chase; lanes *3* and *10*, 15-min chase; lanes *4* and *11*, 30-min chase; lanes *5* and *12*, 45-min chase; lanes *6* and *13*, 1 h chase; lanes *7* and *14*, 2 h chase. The lower band in the cell lysates (*C*) is the capsid protein of SFV.

of cell lysates were directly analyzed by SDS-PAGE, whereas extracellular particles were first concentrated by pelletation through a sucrose cushion. Proportionally five times more of medium samples were loaded on the gel. As can be seen in Fig. 1, lanes *8–14*, labeled Pr65^{gag} was first detected in extracellular particles at the 15-min chase point, and most of Pr65^{gag} was released between 15 min and 45 min of chase. Maximum release was reached after 2 h of chase (data not shown). Quantitations indicated that ~31% of synthesized Pr65^{gag} was released into extracellular particles during the 2 h chase (data not shown). Thus, it can be concluded that the Pr65^{gag} expressed from the recombinant SFV-C/Pr65gag-genome is efficiently incorporated into extracellular particles, and therefore this expression system can be used as a model to study targeting of newly synthesized Pr65^{gag} to the cell surface.

Inhibitors of the Secretory Pathway Do Not Block the Incorporation of Newly Synthesized M-MuLV Gag into Extracellular Particles

BFA, monensin, and 20°C-block are well-characterized inhibitors of the secretory pathway that block the forward vesicular traffic from ER, from medial-Golgi and from TGN, respectively (15, 16, 23, 55). As a first test towards determining whether the secretory pathway is involved in the transport of M-MuLV Gag to the cell surface, we analyzed the effects of these three inhibitors on the release of newly synthesized Pr65^{gag} from cells.

Fig. 2 *a* shows the release of Pr65^{gag} from SFV-C/Pr65gag–infected cells in the presence and absence of 10 μg/ml BFA. At 4.5 h postinfection cells were metabolically labeled with [^{35}S]methionine for 10 min and chased for 5 min or 2 h, and the amount of Pr65^{gag} in cell lysates and extracellular particles was determined as described for Fig. 1. BFA was added to cells 30 min before the pulse and maintained throughout the pulse and chase. By comparing lanes *4* and *8* in Fig. 2 *a*, it is evident that Pr65^{gag} was released as efficiently from BFA-treated cells as from mock-treated cells during the 2 h chase. This strongly suggested that the newly synthesized Pr65^{gag} is not initially inserted into the ER. To ensure that the concentration of BFA used was sufficient to block the vesicular traffic from the ER, parallel plates were infected with wild-type SFV, and the transport of the viral spike protein complex to the cell surface was analyzed in the presence and absence of 10 μg/ml BFA. The SFV spike complex is composed of two integral membrane proteins, p62 and E1, which form a heterodimeric complex in the ER (29, 59, 67). After exit of the spike complex from the TGN, the p62-subunit is cleaved by a host protease in its external domain to yield the E2 form found in mature virions (8). SFV-infected cells were pulse-labeled for 10 min, chased for 5 min to 3 h, and after the chase, externally exposed plasma membrane–associated proteins were labeled by biotinylation at 4°C before detergent solubilization of cells. Biotinylated proteins were precipitated from cell lysates by streptavidin-agarose. Analysis of total cell lysates and streptavidin-precipitated proteins is shown in Fig. 2, *b* and *c*, respectively. In the absence of BFA, the p62 subunit of the spike complex was efficiently converted to the E2 form, which, in the gel system used, comigrates with E1 (Fig. 2 *b*, lanes *1–3*). Starting from the 1.5-h chase point the spike complex could be detected at the cell surface (Fig. 2 *c*, lanes *1–3*). In contrast, in the presence of BFA processing of p62 to E2 was inhibited (Fig. 2 *b*, lanes *4–6*), and no spike complexes were captured by streptavidin-precipitation (Fig. 2 *c*, lanes *4–6*). Therefore, it can be concluded that the concentration of BFA used was sufficient to block the transport of proteins from the ER.

To test the effect of monensin on the release of newly synthesized Pr65^{gag}, SFV-C/Pr65gag–infected cells were pulse-labeled and chased in the presence and absence of 5 μM monensin as described for the BFA experiment. Analysis of total cell lysates and extracellular particles is shown in Fig. 3 *A*. By comparing the amount of Pr65^{gag} in particles released from mock-treated (lane *4*) and monensin-treated (lane *8*) cells after 2 h of chase, it is evident that monensin had no effect on incorporation of Pr65^{gag} into extracellular particles. The monensin concentration used was sufficient to inhibit vesicular traffic from medial-Golgi, since in monensin-treated, wild-type SFV-infected control cells, processing of p62 to E2 was severely compromised and only small amounts of spike proteins could be detected at the cell surface after 3 h of chase (Fig. 3, *B* and *C*, respectively).

To analyze whether inhibition of protein transport from TGN blocks release of newly synthesized Pr65^{gag}, SFV-C/Pr65gag–infected cells were shifted to 20°C at 4 h postinfection, and after 30 min cells were pulse-labeled and chased at 20°C as described for the BFA experiment. Control cells were shifted back to 37°C after the pulse. Since the rate of protein synthesis is slower at 20°C, and consequently also the incorporation of label into Pr65^{gag} is less efficient, it was necessary to concentrate Pr65^{gag} from cell lysates by immunoprecipitation before gel analysis. As shown in Fig. 4 *A*, incubation at 20°C did not block incorporation of labeled Pr65^{gag} into extracellular particles. Slightly fewer particles were present at the extracellular medium after 2 h of chase at 20°C as compared to chase at

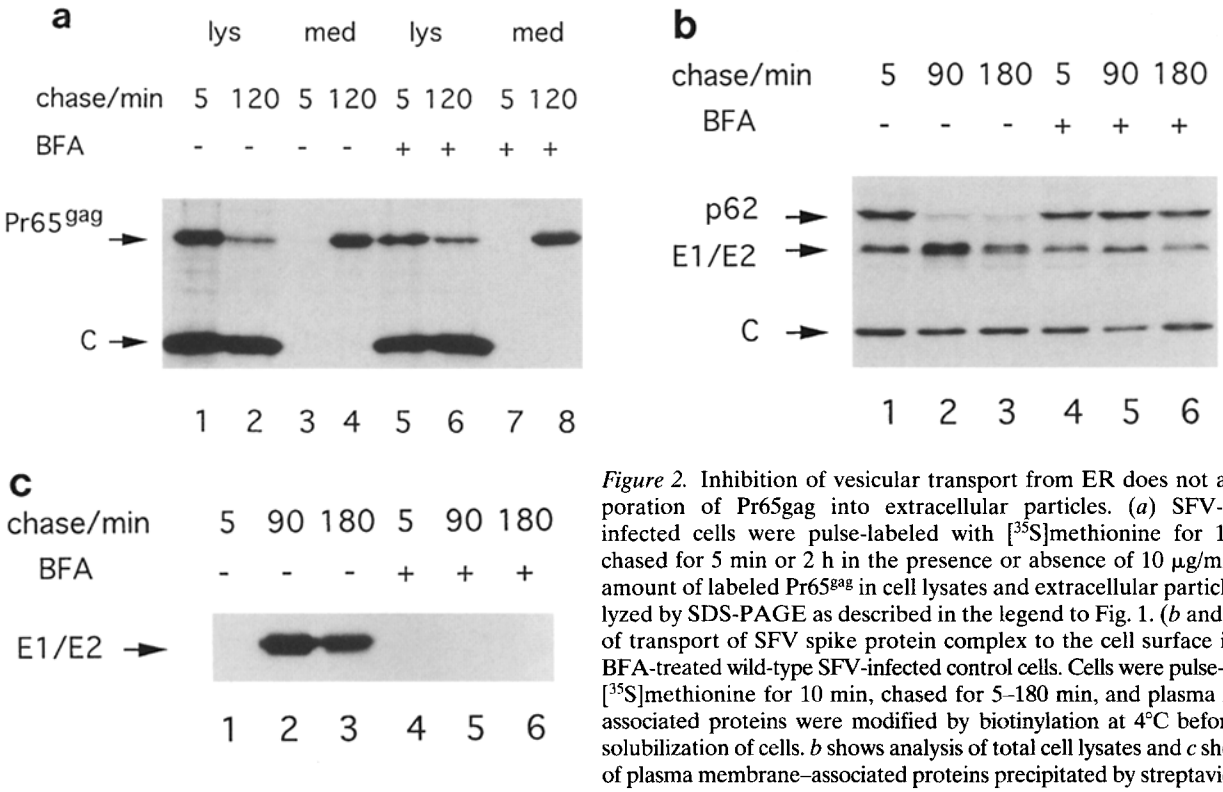

Figure 2. Inhibition of vesicular transport from ER does not affect incorporation of Pr65gag into extracellular particles. (*a*) SFV-C/Pr65gag–infected cells were pulse-labeled with [^{35}S]methionine for 10 min and chased for 5 min or 2 h in the presence or absence of 10 μg/ml BFA. The amount of labeled Pr65^{gag} in cell lysates and extracellular particles was analyzed by SDS-PAGE as described in the legend to Fig. 1. (*b* and *c*) Analysis of transport of SFV spike protein complex to the cell surface in mock- or BFA-treated wild-type SFV-infected control cells. Cells were pulse-labeled with [^{35}S]methionine for 10 min, chased for 5–180 min, and plasma membrane–associated proteins were modified by biotinylation at 4°C before detergent solubilization of cells. *b* shows analysis of total cell lysates and *c* shows analysis of plasma membrane–associated proteins precipitated by streptavidin-agarose.

37°C, but this difference is most likely due to a direct effect of the temperature on the budding process itself, since a more detailed pulse-chase analysis indicated that the kinetics of release of Gag particles was slower at 20°C than at 37°C (data not shown). The 20°C block was effective in blocking vesicular transport from TGN, since in the SFV-infected control cells, transport of the viral spike complex to the cell surface was inhibited at 20°C, as evidenced by the inefficient processing of p62 to E2 (Fig. 4 *B*) and by the inability to detect spike proteins at the cell surface by biotinylation (Fig. 4 *C*).

Taken together these BFA-, monensin- and 20°C block results strongly suggested that Pr65^{gag} that is released from cells does not initially associate with internal membranes, but instead is directly inserted into the plasma membrane.

Analysis of Intracellular Targeting of M-MuLV Gag by Subcellular Fractionation

To obtain more concrete evidence for direct insertion of M-MuLV Gag into the plasma membrane, we turned to subcellular fractionations. Kinetics and efficiency of membrane association of newly synthesized Pr65^{gag} was first determined. At 4.5 h postinfection SFV-C/Pr65gag–infected cells were metabolically labeled with [^{35}S]methionine for 5 min and chased for 0 min to 30 min. Postnuclear supernatant (PNS) fractions of total cell homogenates were mixed with 70% (wt/wt) sucrose, placed at the bottom of a step gradient consisting of 65% (wt/vol) and 10% (wt/vol) sucrose, and membranes were fractionated by equilibrium flotation during ultracentrifugation. Membranes float to the 65–10% sucrose interphase (fraction 1), whereas soluble proteins remain at the bottom of the tube (fractions 3–5). Although Pr65^{gag}, like other myristoylated proteins, was expected to be synthesized on free ribosomes in the cytoplasm (21), to our surprise we could never detect a clear initial soluble pool for Pr65^{gag}. As can be seen in Fig. 5, already at the 0-min chase point the majority of total Pr65^{gag} (~64%) was found in fraction 1, and after a 15-min chase, the membrane-bound pool of Pr65^{gag} had increased to ~80%. The lower amount of label in Pr65^{gag} at the 0-min chase point is most likely due to the fact that incorporation of label into proteins continues for a short while after the onset of chase. The Pr65^{gag} proteins found in fraction 1 at the 0-min chase point display characteristics of proteins firmly associated with membranes. When a sample of this fraction was treated with EDTA (50 mM), high salt (2 M KCl) or high pH (100 mM Na_2CO_3) and subjected to recentrifugation, 70–79% of total Pr65^{gag} again floated up to the membrane fraction (84% of total Pr65^{gag} floated up in the mock-treated sample; data not shown). The gradient used was capable of properly separating cytosolic material from membranes, because the soluble SFV C protein was only found in the bottom fractions. Taken together these results indicated that the newly synthesized Pr65^{gag} binds to membranes very rapidly and very efficiently.

To determine the identity of the membranes that harbor the newly synthesized Pr65^{gag}, a modification of the sucrose step gradient described by Saraste et al. (49) was used. The TRΔ2-mutant of human transferrin receptor was used as a marker for the ER and the plasma membrane (53). This is a type II integral membrane protein which is synthesized in the rough ER and then transported to the plasma membrane. Contrary to its wild-type coun-

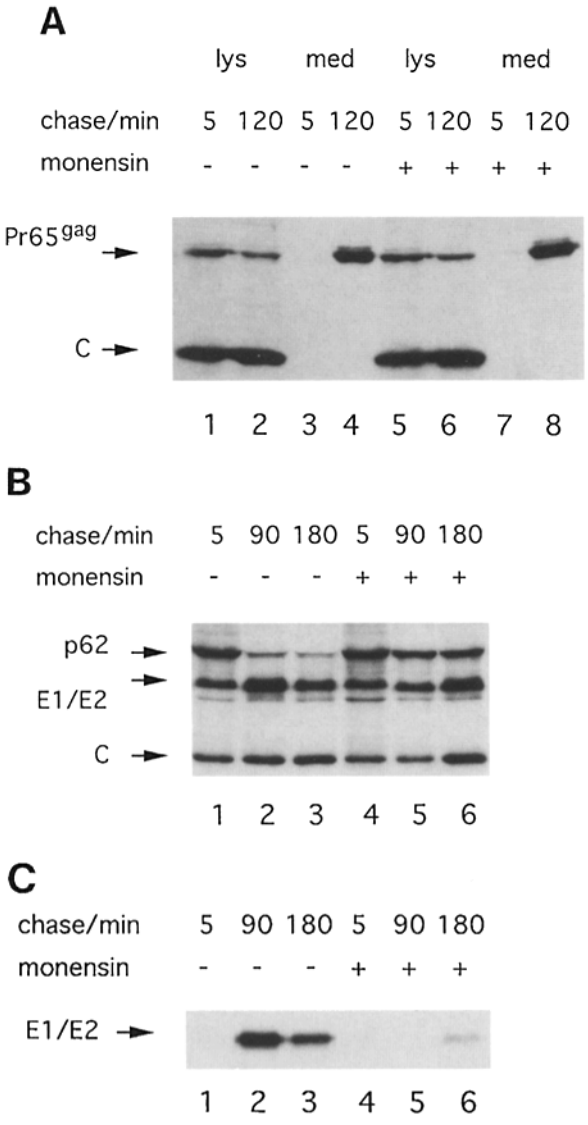

Figure 3. Inhibition of vesicular transport at the level of medial-Golgi does not block incorporation of Pr65^{gag} into extracellular particles. (*A*) SFV-C/Pr65gag–infected cells were pulse-labeled with [^{35}S]methionine for 10 min and chased for 5 min or 2 h in the presence or absence of 5 μM monensin. The amount of labeled Pr65^{gag} in cell lysates and extracellular particles was analyzed by SDS-PAGE as described in the legend to Fig. 1. (*B* and *C*) Analysis of transport of SFV spike protein complex to the cell surface in mock- or monensin-treated wild-type SFV-infected control cells. Cells were processed and analyzed as described in the legend to Fig. 2. (*B*) Total cell lysates. (*C*) Streptavidin-precipitated proteins.

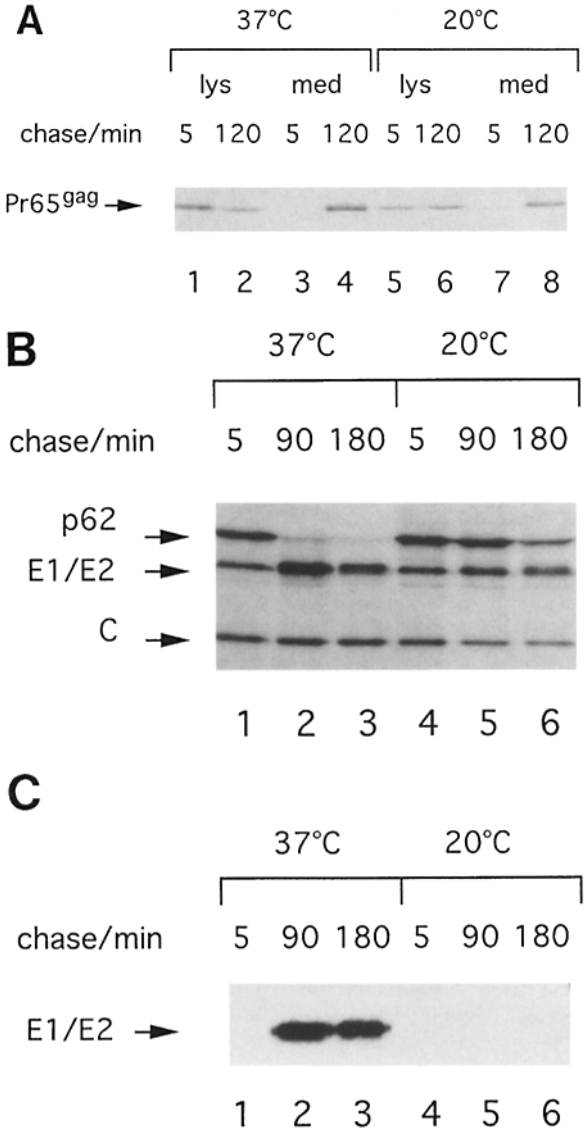

Figure 4. Inhibition of protein transport from TGN does not block incorporation of Pr65^{gag} into extracellular particles. (*A*) SFV-C/Pr65gag–infected cells were pulse-labeled with [^{35}S]methionine for 10 min at 20°C and chased either at 20°C or at 37°C for 5 min or 2 h. Lysate and media samples were analyzed as described in the legend to Fig. 1, except that Pr65^{gag} proteins were immunoprecipitated from cell lysates before gel analysis. (*B* and *C*) Analysis of transport of SFV spike protein complex to the cell surface in wild-type SFV-infected control cells incubated at 20°C or at 37°C. Cells were pulse-labeled at 37°C for 10 min, subsequently chased either at 20°C or at 37°C for 5-180 min and processed as described in the legend to Fig. 2. (*B*) Total cell lysates. (*C*) Streptavidin-precipitated proteins.

terpart, TRΔ2 does not undergo endocytosis and recycling due to a deletion in its cytoplasmic tail that has removed the endocytosis signal (7). The newly synthesized form of the TRΔ2 was used as a marker for ER. BHK-21 cells were infected with a recombinant SFV-genome expressing TRΔ2 (53), and PNS fractions were prepared from cells after a 10-min pulse and 5-min chase. As shown in Fig. 6 *A*, the major peak of radioactively labeled TRΔ2 was found in fraction 8, at the density of 1.217 g/ml. Upon transport to the plasma membrane, TRΔ2 is converted to a slower migrating form (38, 53), and this form was used as a marker for the plasma membrane. The slower migrating form of TRΔ2 truly represents the cell surface–associated fraction of the protein, because essentially all of it is accessible to exogenously added protease (data not shown). To obtain enough signal into this form, TRΔ2-expressing cells were pulsed for 20 min and chased for 3 h. As shown in Fig. 6 *A*, the slower migrating TRΔ2 form was fairly broadly distributed along the gradient, with a major peak

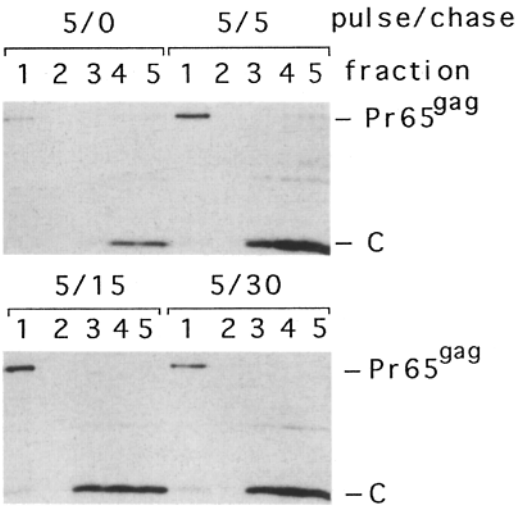

Figure 5. Kinetics and efficiency of membrane binding of newly synthesized Pr65^{gag}. SFV-C/Pr65gag–infected cells were pulse-labeled with [^{35}S]methionine for 5 min and chased for 0 min, 5 min, 15 min, or 30 min. Postnuclear supernatant fractions of total cell homogenates were mixed with 70% (wt/wt) sucrose, and overlaid with 65% (wt/vol) and 10% (wt/vol) sucrose layers, and membrane-associated proteins were separated from soluble ones by equilibrium flotation during ultracentrifugation. Fractions were collected from the top and aliquots of fractions were analyzed by SDS-PAGE. Membrane-associated proteins are found in fraction 1 and soluble cytoplasmic proteins in fractions 3–5. The lower band (*C*) is the capsid protein of SFV.

in fractions 3–5 (between densities 1.136–1.164 g/ml). Similar results were obtained when PNS fractions prepared from SFV-C/TRΔ2- and SFV-C/Pr65gag–coinfected cells were analyzed (data not shown). The faster migrating 'ER'-form of TRΔ2 is still identifiable in fraction 8, being the lower of the two bands. The broad distribution of the slower migrating TRΔ2 on the gradient was not unexpected, because it is a known property of the plasma membrane to break into vesicles of varying density during homogenization (e.g., 49). When the activity of galactosyl transferase, a marker for the *trans*-Golgi, was analyzed in the gradient fractions, the major peak of activity was found in fraction 3, at the density 1.136 g/ml (data not shown).

To determine what membranes Pr65^{gag} is inserted into, SFV-C/Pr65gag–infected cells were pulse-labeled for 10 min and chased for 0 min to 1 h. As shown in Fig. 6 *B*, immediately after the pulse the majority of labeled Pr65^{gag} was found in fractions 3–5. This distribution overlapped the distribution of the plasma membrane marker, and most importantly, the peak of Pr65^{gag} was clearly resolved from the ER marker, and also separated from the peak of galactosyl transferase activity (see above). Thus, these results are consistent with direct insertion of Pr65^{gag} into the plasma membrane. After 30 min of chase a slight change in the distribution Pr65^{gag} was evident; labeled Pr65^{gag} had disappeared from fraction 3 and the majority of Pr65^{gag} was now found in fractions 4–6, between densities 1.156–1.178 g/ml. This change however was not due to vesicular transport of Pr65^{gag} from one membrane organelle to another, because a similar change was also observed under

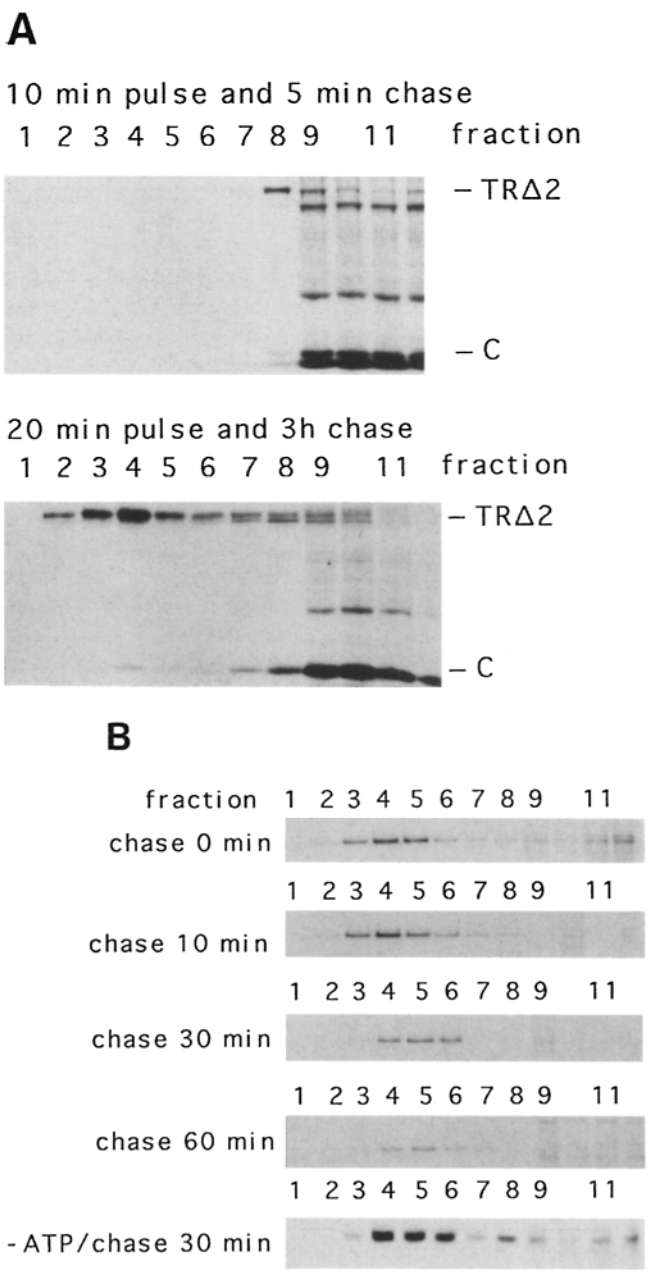

Figure 6. Distribution of Pr65^{gag} in subcellular fractions of SFV-C/Pr65gag–infected cells. (*A*) Gradient profiles of the TRΔ2-mutant of human transferrin receptor used as a marker for the ER and the plasma membrane. Postnuclear supernatants of SFV-C/TRΔ2–infected cell homogenates prepared after a 10-min pulse and a 5-min chase (ER-marker) or after a 20-min pulse and 3 h chase (plasma membrane marker) were mixed with 65% (wt/wt) sucrose and overlaid with 53%, 40%, 35%, 30%, and 10% (all wt/wt) sucrose layers, and membranes were fractionated by equilibrium flotation during ultracentrifugation. Fractions were collected from the top and aliquots of fractions were analyzed by SDS-PAGE. The band marked *C* is the capsid protein of SFV. (*B*) Analyses of postnuclear supernatant fractions of SFV-C/Pr65gag–infected cells on similar gradients. Cells were pulse-labeled for 10 min and chased for 0 min to 1 h. Shown is only the part of the gel that contained labeled Pr65^{gag}-band. Last panel (marked-ATP) is from a separate experiment and shows distribution of Pr65^{gag} after 30 min of chase under conditions of ATP depletion.

conditions of ATP depletion (Fig. 6 *B*), i.e., under conditions when all vesicular transport is inhibited (40). Under ATP depletion, however, no labeled $Pr65^{gag}$ was released into the culture medium, thereby indicating that budding (or completion of the budding reaction) was inhibited under these conditions (data not shown). The time-dependent disappearance of labeled $Pr65^{gag}$ from fraction 3 could represent incorporation of $Pr65^{gag}$ into budding structures, since when extracellular Gag particles are analyzed on similar gradients and they band in fractions 4 and 5 (data not shown). Furthermore, when gradient fractions were analyzed by electron microscopy, budding structures were clearly identifiable in fractions 4 and 5 (data not shown). With longer chase times there was also a clear decrease in the overall intensity of $Pr65^{gag}$ bands. This decrease correlated with release of labeled $Pr65^{gag}$ into culture media (data not shown).

The above described membrane fractionation studies not only indicated that the newly synthesized $Pr65^{gag}$ is directly inserted into the plasma membrane, but they also suggested that the membrane insertion reaction is strikingly specific. However, since medial- and *cis*-Golgi elements also band at densities 1.13–1.15 g/ml (27, 49), the gradient analyses could not completely exclude the possibility that some $Pr65^{gag}$ in fractions 3–5 represented proteins targeted to these Golgi elements. This possibility appears unlikely in view of the monensin and 20°C block experiments described above. However, to firmly establish that the bulk of $Pr65^{gag}$ is specifically inserted into the plasma membrane, we further investigated the subcellular localization of the protein by protease protection analysis and by electron microscopy.

Newly Synthesized $Pr65^{gag}$ Is Protease-protected in Cell Homogenates

Homogenization of the plasma membrane predominantly yields vesicles with "right-side out"-orientation (e.g., 10), and therefore $Pr65^{gag}$ bound to the cytoplasmic leaflet of the plasma membrane is expected to be protease-resistant unless the membrane is dissolved by detergents. On the other hand, $Pr65^{gag}$ inserted into the cytoplasmic leaflet of the Golgi is expected to be protease sensitive, unless budding into this compartment has occurred. To investigate the protease-sensitivity of newly synthesized $Pr65^{gag}$ in cell homogenates, we pulse-labeled SFV-C/Pr65gag–infected cells for 10 min and chased for 2 min before homogenization and protease treatment. As shown in Fig. 7, $Pr65^{gag}$ was protected from exogenously added proteinase K in the absence of detergent, whereas in the presence of 1% NP-40 the protein became protease-sensitive. To rule out the possibility, however unlikely, that some of the protease resistance of $Pr65^{gag}$ was due to rapid intracellular budding, the Golgi and plasma membrane of SFV-C/Pr65gag–infected cells were examined for the presence of budding profiles by electron microscopy. Sections of the plasma membrane and Golgi of a typical-infected cell is shown in Fig. 8 *A* and Fig. 8 *B*, respectively. M-MuLV–like budding profiles were abundant at the cell surface. These were at different stages of maturation and showed a typical double-layered surface morphology. In contrast, no Golgi-associated budding profiles or particles could be detected. Furthermore, when subcellular distribution of $Pr65^{gag}$ was analyzed by immunoelectron microscopy using a polyclonal anti-p30 antiserum directed against the capsid-domain of $Pr65^{gag}$ and detected with protein A conjugated with 10 nm gold, concentration of gold particles was found to be fourfold higher at the plasma membrane than in the cell interior (data not shown). Thus, taken together, these results confirmed that the bulk of $Pr65^{gag}$ is specifically inserted into the plasma membrane.

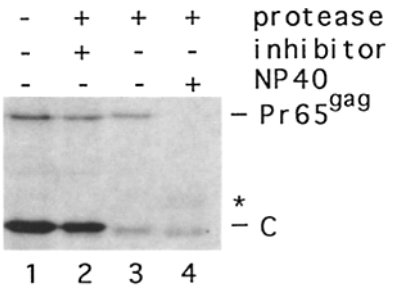

Figure 7. Newly synthesized $Pr65^{gag}$ is protease-resistant in cell homogenates. SFV-C/Pr65gag–infected cells were pulse-labeled with [^{35}S]methionine for 10 min and chased for 2 min. Aliquots of PNS fractions of crude cell homogenates were treated with proteinase K (marked protease) in the presence and absence of protease-inhibitor phenylmethylsulfonyl fluoride (marked inhibitor), or in the presence and absence of 1% NP-40 (NP-40). The lower band (*C*) is the capsid protein of SFV. Asterisk (*) indicates a proteolytic product of $Pr65^{gag}$.

Discussion

The core protein precursor Gag is the principle actor in retroviral budding reactions at the cell surface (9, 12, 48, 53, 62). After their synthesis most retroviral Gag proteins become anchored into the cytoplasmic leaflet of the plasma membrane via a dual motif consisting of an amino-terminal myristic acid and a cluster of basic amino acids (6, 9, 12, 47, 64, 66). In this work we have studied the mechanism by which these myristoylated Gag precursors are targeted to the plasma membrane using M-MuLV Gag as an example. Our results indicate that the newly synthesized M-MuLV Gag is directly inserted into the plasma membrane, and that the membrane insertion reaction is highly efficient and highly specific. These conclusions are based on three lines of evidence. First, the well characterized inhibitors of the secretory pathway, BFA, monensin, and 20°C block, did not inhibit the incorporation of newly synthesized Gag precursors into extracellular particles, thereby ruling out the involvement of the secretory pathway in the transport of Gag to the cell surface. Second, subcellular fractionation studies demonstrated that immediately after synthesis, essentially all Gag was found in light membranes that had densities similar to those of plasma membrane–derived vesicles. Third, protease-protection studies on crude cell homogenates confirmed that these Gag-containing membranes indeed were of plasma membrane origin, since the newly synthesized Gag was found to be sequestered inside membrane vesicles, as expected of a protein that binds to the cytoplasmic leaflet of the plasma membrane. The other explanation for the ob-

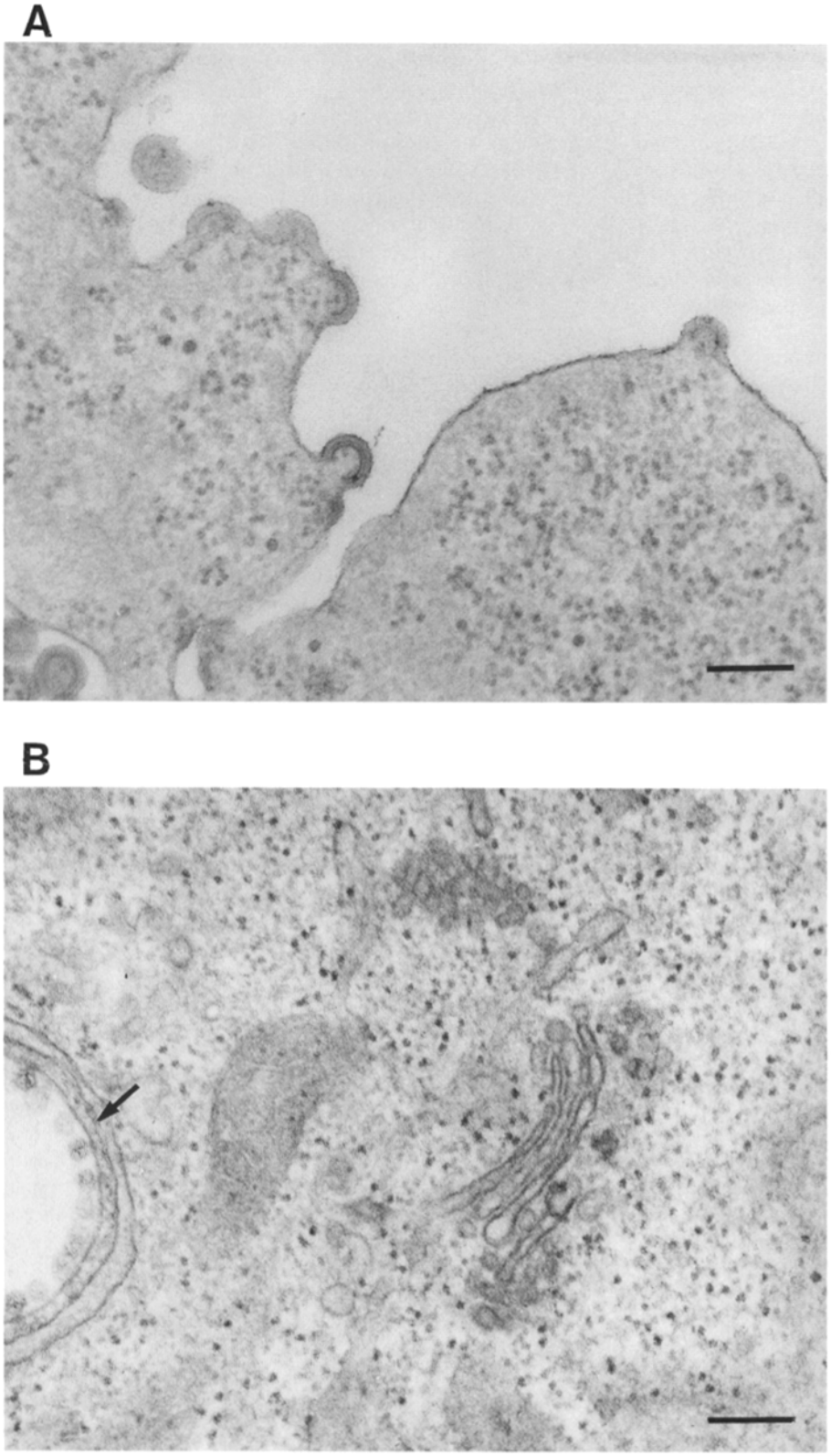

Figure 8. EM-analysis of SFV-C/Pr65gag–infected cells. (*A*) A typical view of the plasma membrane of a SFV-C/Pr65gag–infected cell. (*B*) A section of the cytoplasm of the same cell showing Golgi membranes; in contrast to the plasma membrane, the Golgi membranes are devoid of M-MuLV budding profiles or particles. A characteristic type I cytopathic vacuole of SFV-infected cells can be seen on the left hand side of the figure (indicated by an arrow). This type I cytoplasmic vacuole is the site of viral RNA replication in SFV-infected cells. Bars, 200 nm.

served protease resistance of newly synthesized Gag, namely rapid intracellular budding, was ruled out by EM analysis of Gag-expressing cells; in these analyses budding profiles or budded particles were observed only at the plasma membrane, not in the ER or Golgi. Although the results were obtained by using a heterologous expression system, we believe the conclusions are valid for wild-type M-MuLV–infected cells as well, because also in these cells the majority of Gag (~65%) is found in light membrane vesicles after a 20-min pulse and a 2-min chase (the shortest pulse-label-

ing conditions to give quantifiable signal) and these vesicles band at the same density as the Gag-containing vesicles of the present study (Suomalainen, M., unpublished).

There are two previous reports, which contrary to our results, suggested that M-MuLV Gag precursors are targeted to the plasma membrane via the secretory pathway and that the membrane insertion of M-MuLV Gag is not restricted to the plasma membrane. Hansen et al. (18) postulated that at least a portion of newly synthesized M-MuLV Gag travels to the cell surface via vesicular transport since they found that monensin decreases yields of extracellular M-MuLV particles. However, the monensin concentrations used in that study were five times higher than in the present study, and over a 6 h incubation period, this concentration only produced about a threefold reduction in the number of extracellular particles. Considering the toxicity of monensin and the longer incubation period, the decrease in particle production could have resulted from effects other than a block in the secretory pathway. In agreement with our results, Krishna et al. (26) recently reported that blocking the vesicular traffic from ER by BFA does not inhibit release of M-MuLV particles from wild-type M-MuLV–infected cells. In another paper, Hansen et al. (17) provided evidence for intracellular budding of M-MuLV in 3T3 cells thereby suggesting that the M-MuLV Gag is not specifically inserted into the plasma membrane. However, the evidence was based on electron microscopic analysis alone, and therefore no proper conclusions could be drawn about the relative efficiencies with which Gag was targeted to the plasma membrane vs other membrane compartments. In our SFV-C/Pr65gag–infected BHK-21 cells, we did not observe any intracellular budding of M-MuLV Gag by EM. One possible explanation for these different results is that we used a transient expression system, whereas Hansen et al. (17) used cell lines stably expressing the M-MuLV proteins. In the latter case, the observed intracellular particles could have represented particles accumulated over a longer period of time. Our subcellular fractionation studies strongly suggest that Gag precursors targeted to the intracellular membranes would represent only a minor proportion of total Gag, a proportion that was undetectable in our assays. However, it cannot be excluded that the efficiency of targeting of M-MuLV Gag to the cell surface might vary in different cell lines.

The observed highly efficient and specific targeting of M-MuLV Gag to the plasma membrane is intriguing, because the presumed membrane anchor of Gag, i.e., myristate plus cluster of basic amino acids, is not expected to confer specific insertion into the plasma membrane. Myristoylated proteins in general are found in several cellular compartments (56) and acidic phospholipids are not restricted to the plasma membrane either (39, 57). The most simple explanation for our results is that the membrane insertion of M-MuLV Gag is dependent on an as-yet-unidentified cellular factor (or factors). There are at least two ways that these factors could operate. First, the putative cellular factor(s) could be a plasma membrane–associated Gag "receptor" protein, which increases the affinity of Gag to the plasma membrane either via stoichiometric protein–protein interactions or via a catalytic interaction. There is a precedent in literature for the latter type of receptor interaction in the targeting of a myristoylated protein to a specific membrane compartment: the small GTP-binding protein ARF1 (ADP-ribosylation factor 1), which binds to membranes in its GTP-bound form but not in its GDP-bound form, is targeted to Golgi by interaction of ARF1 with a Golgi membrane enzyme that catalyzes exchange of GDP for GTP on ARF1 (11, 20). If targeting of M-MuLV Gag to the plasma membrane is dependent on an interaction with a plasma membrane–associated receptor, our unpublished results suggest that the putative receptor interaction is unlikely to be stoichiometric (i.e each Gag molecule engaging in receptor interaction). This is based on the observation that Gag particles released from SFV-C/Pr65gag–infected cells do not contain any cellular proteins in near molar ratios to Gag (Wallengren, K., and H. Garoff, unpublished results). However, it is possible that the specific insertion of M-MuLV Gag into the plasma membrane is directed by two different kinds of protein–protein interactions. Since Gag precursors have a high propensity for self-oligomerization, it is possible that initially only a few molecules of Gag are required to interact with a plasma membrane–associated receptor and the subsequent recruitment of additional Gag precursors then proceeds via specific Gag–Gag interactions. It is also possible that the putative receptor interaction is catalytic rather than stoichiometric. For example, the amino-terminal myristic acid on a newly synthesized Gag could be unavailable for membrane insertion and a conformational change on the protein is needed for the exposure of the occluded myristoyl moiety. Specific targeting to the plasma membrane could be achieved if this conformational change was brought about by a modification catalyzed by a plasma membrane–associated enzyme. However at present it is unclear what this catalytic modification on M-MuLV Gag could be. According to the second model, Gag is synthesized at, or close to, the plasma membrane. One striking feature of the membrane insertion of Gag was the rapidity of the reaction: already after a 5-min pulse and 0-min chase, the majority of labeled Gag was membrane-bound, and we could not detect a clear initial soluble pool for the protein. This is in contrast to the membrane insertion of the cellular myristoylated protein src tyrosine kinase, which localizes to endosomes and focal adhesions at the plasma membrane; in this case the protein is first found in a soluble pool and becomes membrane associated only after 5 min of chase (28). The rapidity of the membrane insertion of M-MuLV Gag raises the possibility that the reaction occurs cotranslationally instead of posttranslationally. Note that contrary to other myristoylated proteins, the majority of mRNAs encoding the Gag precursor of another murine leukemia virus, the Rauscher murine leukemia virus, have been reported to be membrane-bound (13, 14). Localization of Gag-encoding mRNAs to close proximity of the plasma membrane could explain the observed rapid and specific insertion of M-MuLV Gag into the plasma membrane. This localization could be achieved via specific targeting and/or anchoring of Gag-encoding mRNAs to the cytoskeletal elements underneath the plasma membrane. Although there are yet no examples of specific localization of mRNAs in nonpolarized cells, targeting of mRNAs to specific sites in eggs, oocytes, and polarized somatic cells is emerging as an important mechanism for targeting of cytosolic proteins in these cells (for reviews see references 52, 60).

Presumably, the route of M-MuLV Gag to the plasma membrane, i.e., direct insertion, is shared by Gag precursors of other retroviruses as well, since, e.g., monensin and BFA do not affect release of HIV-1 and Rous sarcoma virus Gag precursors from cells (26, 42, 43). In the case of Rous sarcoma virus, the Gag precursor is not myristoylated, but instead carries an acetyl-group at its amino-terminus (44). Interestingly, contrary to the M-MuLV Gag, when the HIV-1 Gag is expressed from a recombinant SFV genome, it becomes less efficiently membrane-associated (Hewson, R., and H. Garoff, unpublished results). This suggests that the membrane insertion reaction of HIV-1 Gag might be dependent on some additional viral protein(s). In polarized epithelial cells the intracellular targeting of HIV-1 Gag can apparently be modulated by viral spike proteins. However, when Gag is coexpressed with viral spike proteins, the particle formation shifts mainly to the basolateral surface, that is the same domain where vital spike proteins are targeted (32, 41). Therefore, the possibility that efficient membrane interaction of HIV-1 Gag requires viral spike proteins cannot be excluded at present. It is clear from our results that viral spike proteins are dispensable for efficient membrane insertion of M-MuLV Gag, but understanding the molecular basis of this membrane insertion will require in vitro reconstitution of the reaction.

The authors would like to thank Dr. Roger Hewson for critical reading of the manuscript, and Maria Karlsson and Kristina Wallengren for their contributions to the pilot experiments of this work.

This work was supported by grants from the European Union (CHRX-CT94-0496 and CHRX-CT92-0018), the Swedish Natural Science Research Council (B-BU-09353-310), and the Swedish Cancer Society (3277-B93-02XBB).

Received for publication 15 July 1996 and in revised form 16 September 1996.

References

1. Aliperti, G., and M.J. Schlesinger. 1978. Evidence for an autoprotease activity of Sindbis virus capsid protein. *Virology.* 90:366–369.
2. Allison, S.L., K. Stadler, C.W. Mandl, C. Kunz, and F.X. Heinz. 1995. Synthesis and secretion of recombinant tick-borne encephalitis virus protein E in soluble and particulate form. *J. Virol.* 69:5816–5820.
3. Braakman, I., J. Helenius, and A. Helenius. 1992. Role of ATP and disulphide bonds during protein folding in the endoplasmic reticulum. *Nature (Lond.).* 356:260–262.
4. Brew, K., J. Shaper, K.W.Q. Olsen, I.O. Trayer, and R.L. Hill. 1975. Cross-linking of the components of lactose synthetase with dimethylpimelimidate. *J. Biol. Chem.* 250:1434–1444.
5. Bruss, V., and D. Ganem. 1991. The role of envelope proteins in hepatitis B virus assembly. *Proc. Natl. Acad. Sci. USA.* 88:1059–1063.
6. Bryant, M. L., and L. Ratner. 1990. Myristylation-dependent replication and assembly of Human immunodeficiency virus 1. *Proc. Natl. Acad. Sci. USA.* 87:523–527.
7. Collawn, J.F., M. Stangel, L.A. Kuhn, V. Esekogwu, S. Jing, I.S. Trowbridge, and J.A. Tainer. 1990. Transferrin receptor internalization sequence YXRF implicates a tight turn as the structural recognition motif for endocytosis. *Cell.* 63:1061–1072.
8. de Curtis, I., and K. Simons. 1988. Dissection of Semliki Forest virus glycoprotein delivery from the *trans*-Golgi network to the cell surface in permeabilized BHK cells. *Proc. Natl. Acad. Sci. USA.* 85:8052–8056.
9. Delchambre, M., D. Gheysen, D. Thines, C. Thiriart, E. Jacobs, E. Verdin, M. Horth, A. Burny, and F. Bex. 1989. The GAG precursor of Simian Immunodeficiency virus assembles into virus-like particles. *EMBO (Eur. Mol. Biol. Organ.) J.* 8:2653–2660.
10. Devaney, E., and K. E. Howell. 1985. Immuno-isolation of a plasma membrane fraction from the Fao cell. *EMBO (Eur. Mol. Biol. Organ.) J.* 4: 3123–3130.
11. Donaldson, J.G., D. Finazzi, and R.D. Klausner. 1992. Brefeldin A inhibits Golgi-catalyzed exchange of guanine nucleotide onto ARF proteins. *Nature (Lond.).*. 360:350–352.
12. Gheysen, D., E. Jacobs, F. de Frosta, C. Thiriart, M. Francotte, D. Thines, and M. De Wilde. 1989. Assembly and release of HIV-1 precursor Pr55gag virus-like particles from recombinant Baculovirus-infected cells. *Cell.* 59:103–112.
13. Gielkens, A. L. J., M. H. L. Salden, and H. Bloemendal. 1974. Virus-specific messenger RNA on free and membrane-bound polyribosomes from cells infected with Rauscher leukemia virus. *Proc. Natl. Acad. Sci. USA.* 71:1093–1097.
14. Gielkens, A.L.J., D. Van Zaane, H.P.J. Bloemers, and H. Bloemendal. 1976. Synthesis of Rauscher murine leukemia virus-specific polypeptides in vitro. *Proc. Natl. Acad. Sci. USA.* 73:356–360.
15. Griffiths, G., and K. Simons. 1986. The *trans*-Golgi Network: sorting at the exit site of the Golgi complex. *Science (Wash. DC).*. 234:438–443.
16. Griffiths, G., P. Quinn, and G. Warren. 1983. Dissection of the Golgi complex. I. Monensin inhibits the transport of viral membrane proteins from medial to *trans*-Golgi cisternae in baby hamster kidney cells infected with Semliki Forest virus. *J. Cell Biol.* 96:835–850.
17. Hansen, M., L. Jelinek, R. S. Jones, J. Stegeman-Olsen, and E. Barklis. 1993. Assembly and composition of intracellular particles formed by Moloney murine leukemia virus. *J. Virol.* 67:5163–5174.
18. Hansen, M., L. Jelinek, S. Whiting, and E. Barklis. 1990. Transport and assembly of gag proteins into Moloney murine leukemia virus. *J. Virol.* 64: 5306–5316.
19. Hare, J.F., and E. Lee. 1989. Metabolic behavior of cell surface biotinylated proteins. *J. Cell Biol.* 28:574–580.
20. Helms, J.B., and J.E. Rothman. 1992. Inhibition by brefeldin A of a Golgi membrane enzyme that catalyzed exchange of guanine nucleotide bound to ARF. *Nature (Lond.).*. 360:352–354.
21. Johnson, D.R., R.S. Bhatnagar, L.J. Knoll, and J.I. Gordon. 1994. Genetic and biochemical studies of protein N-myristylation. *Annu. Rev. Biochem.* 63:869–914.
22. Kääriäinen, L., K. Simons, and C.-H. von Bonsdorff. 1969. Studies in subviral components of Semliki Forest virus. *Annu. Med. Exp. Biol. Fenn.* 47: 235–248.
23. Klausner, R.D., J.G. Donaldson, and J. Lippincott-Schwartz. 1992. Brefeldin A: insights into the control of membrane traffic and organelle structure. *J. Cell Biol.* 116:1071–1080.
24. Konishi, E., S. Pincus, E. Paoletti, W.W. Laegreid, R.E. Shope, and P.W. Mason. 1992. Mice immunized with a subviral particle containing the Japanese encephalitis virus prM/M and E proteins are protected from lethal JEV infection. *Virology.* 188:714–720.
25. Krijnse-Locker, J., M. Ericsson, P.J.M. Rottier, and G. Griffiths. 1994. Characterization of the budding compartment of Mouse Hepatitis virus: evidence that transport from RER to the Golgi complex requires only one vesicular transport step. *J. Cell Biol.* 124:55–70.
26. Krishna, N.K., R.A. Weldon, and J.W. Wills. 1996. Transport and processing of the Rous sarcoma virus Gag protein in the endoplasmic reticulum. *J. Virol.* 70:1570–1579.
27. Lahtinen, U., B. Dahllöf, and J. Saraste. 1992. Characterization of a 58 kDa *cis*-Golgi protein in pancreatic exocrine cells. *J. Cell Sci.* 103:321–333.
28. Levinson, A.D., S.A. Courtneidge, and J.M. Bishop. 1980. Structural and functional domains of the Rous sarcoma virus transforming protein ($pp60^{v\text{-}src}$). *Proc. Natl. Acad. Sci. USA.* 78:1624–1628.
29. Liljeström, P., and H. Garoff. 1991. Internally located cleavable signal sequences direct the formation of Semliki Forest virus membrane proteins from a polyprotein precursor. *J. Virol.* 65:147–154.
30. Liljeström, P., and H. Garoff. 1991. A new generation of animal cell expression vectors based on the Semliki Forest virus replicon. *Bio/Technology.* 9:1356–1361.
31. Lisanti, M.P., A. Le Bivic, M. Sargiacomo, and E. Rodriguez-Boulan. 1989. Steady-state distribution and biogenesis of endogenous Madin-Darby canine kidney glycoproteins: evidence for intracellular sorting and polarized cell surface delivery. *J. Cell Biol.* 109:2117–2127.
32. Lodge, R., H. Göttlinger, D. Gabuzda, E.A. Cohen, and G. Lemay. 1994. The intracytoplasmic domain of gp41 mediates polarized budding of Human immunodeficiency virus type 1 in MDCK cells. *J. Virol.* 68:4857–4861.
33. Lopez, S., J.-S. Yao, R.J. Kuhn, E.G. Strauss, and J.H. Strauss. 1994. Nucleocapsid-glycoprotein interactions required for assembly of alphaviruses. *J. Virol.* 68:1316–1323.
34. Mason, P.W., S. Pincus, M.J. Fournier, T.L. Mason, R.E. Shope, and E. Paoletti. 1991. Japanese Encephalitis virus-vaccinia recombinants produce particulate forms of the structural membrane proteins and induce high levels of protection against JEV infection. *Virology.* 180:294–305.
35. McLaughlin, S., and A. Aderem. 1995. The myristoyl-electrostatic switch: a modulator of reversible protein-membrane interactions. *TIBS.* 20:272–276.
36. Mebatsion, T., M. König, and K.-K. Conzelmann. 1996. Budding of rabies virus particles in the absence of the spike glycoprotein. *Cell.* 84:941–951.
37. Melancon, P., and H. Garoff. 1987. Processing of the Semliki Forest virus structural polyprotein: role of the capsid protease. *J. Virol.* 61:1301–1309.
38. Neefjes, J.J., T. Henegveld, O. Tol, and H.L. Ploegh. 1990. Intracellular interactions of transferrin and its receptor during biosynthesis. *J. Cell Biol.* 111:1383–1392.
39. Op den Kamp, J.A.F. 1979. Lipid asymmetry of membranes. *Annu. Rev. Biochem.* 48:47–71.

40. Orci, L., B.S. Glick, and J.E. Rothman. 1986. A new type of coated vesicular carrier that appears not to contain clathrin: its possible role in protein transport within the Golgi stack. *Cell.* 46:171–184.
41. Owens, R.J., J.W. Dubay, E. Hunter, and R.W. Compans. 1991. Human immunodeficiency virus envelope protein determines the site of virus release in polarized epithelial cells. *Proc. Natl. Acad. Sci. USA.* 88:3987–3991.
42. Pal, R., R.C. Gallo, and M.G. Sarngadharan. 1988. Processing of the structural proteins of human immunodeficiency virus type 1 in the presence of monensin and cerulenin. *Proc. Natl. Acad. Sci. USA.* 85:9283–9286.
43. Pal, R., S. Mumbauer, G.M. Hoke, A. Takatsuki, and M.G. Sarngadharan. 1991. Brefeldin A inhibits the processing and secretion of envelope glycoproteins of human immunodeficiency virus type 1. *AIDS Res. Human Retrovir.* 7:707–712.
44. Palmiter, R.D., J. Gagnon, V.M. Vogt, S. Ripley, and R.N. Eisenman. 1978. The NH_2-terminal sequence of the avian oncovirus Gag precursor polyprotein (Pr76gag). *Virology.* 91:423–433.
45. Peränen, J., K. Takkinen, N. Kalkkinen, and L. Kääriäinen. 1988. Semliki Forest virus-specific non-structural protein nsP3 is a phosphoprotein. *J. Gen. Virol.* 69:2165–2178.
46. Pettersson, R.F. 1991. Protein localization and virus assembly at intracellular membranes. *Curr. Top. Microbiol. & Immunol.* 170:67–110.
47. Rein, A., M. McClure, N. Rice, R. Luftig, and A. Schultz. 1986. Myristylation site in Pr65gag is essential for virus particle formation by Moloney murine leukemia virus. *Proc. Natl. Acad. Sci. USA.* 83:7246–7250.
48. Rhee, S., H. Hui, and E. Hunter. 1990. Preassembled capsids of type D retroviruses contain a signal sufficient for targeting specifically to the plasma membrane. *J. Virol.* 64:3844–3852.
49. Saraste, J., G.E. Palade, and M. Gist Farquhar. 1986. Temperature-sensitive steps in the transport of secretory proteins through the Golgi complex in exocrine pancreatic cells. *Proc. Natl. Acad. Sci. USA.* 83:6425–6429.
50. Simon, K., V.R. Lingappa, and D. Ganem. 1988. Secreted Hepatitis B surface antigen polypeptides are derived from a transmembrane precursor. *J. Cell Biol.* 107:2163–2168.
51. Sjöberg, E.M., M. Suomalainen, and H. Garoff. 1994. A significantly improved Semliki Forest virus expression system based on translation enhancer segments from the viral capsid gene. *Bio/Technology.* 12:1127–1131.
52. St. Johnston, D. 1995. The intracellular localization of messenger RNAs. *Cell.* 81:161–170.
53. Suomalainen, M., and H. Garoff. 1994. Incorporation of homologous and heterologous proteins into the envelope of Moloney murine leukemia virus. *J. Virol.* 68:4879–4889.
54. Suomalainen, M., P. Liljeström, and H. Garoff. 1992. Spike protein-nucleocapsid interactions drive the budding of alphaviruses. *J. Virol.* 66:4737–4747.
55. Tartakoff, A.M. 1983. Pertubation of vesicular traffic with the carboxylic ionophore monensin. *Cell.* 32:1026–1028.
56. Towler, D.A., J.I. Gordon, S.P. Adams, and L. Glaser. 1988. The biology and enzymology of eukaryotic protein acylation. *Annu. Rev. Biochem.* 57:69–99.
57. van Meer, G. 1989. Lipid traffic in animal cells. *Annu. Rev. Cell Biol.* 5: 247–275.
58. Vennema, H., G.-J. Godeke, J.W.A. Rossen, W.F. Voorhout, M.C. Horzinek, D.-J.E. Opstelten, and P.J.M. Rottier. 1996. Nucleocapsid-independent assembly of coronavirus-like particles by co-expression of viral envelope protein genes. *EMBO (Eur. Mol. Biol. Organ.) J.* 15:2020–2028.
59. Wahlberg, J.M., W.A. Boere, and H. Garoff. 1989. The heterodimeric association between the membrane proteins of Semliki Forest virus changes its sensitivity to mildly acidic pH during virus maturation. *J. Virol.* 63: 4991–4997.
60. Wilhelm, J.E., and R.D. Vale. 1993. RNA on the move: the RNA localization pathway. *J. Cell Biol.* 123:269–274.
61. Wills, J.W., and R.C. Craven. 1991. Form, function, and use of retroviral Gag proteins. *AIDS.* 5:639–654.
62. Wills, J.W., R.C. Craven, and J.A. Achacoso. 1989. Creation and expression of myristylated forms of Rous sarcoma virus Gag protein in mammalian cells. *J. Virol.* 63:4331–4343.
63. Yamshchikov, V.F., and R.W. Compans. 1993. Regulation of the late events in flavivirus protein processing and maturation. *Virology.* 192: 38–51.
64. Yuan, X., X. Yu, T.-H. Lee, and M. Essex. 1993. Mutations in the N-terminal region of Human immunodeficiency virus type 1 matrix protein block intracellular transport of the Gag precursor. *J. Virol.* 67:6387–6394.
65. Zhao, H., B. Lindqvist, H. Garoff, A. Salminen, C.-H. von Bonsdorff, and P. Liljeström. 1994. A tyrosine-based motif in the cytoplasmic domain of the alphavirus envelope protein is essential for budding. *EMBO (Eur. Mol. Biol. Organ.) J.* 13:4204–4211.
66. Zhou, W., L.J. Parent, J.W. Wills, and M.D. Resh. 1994. Identification of a membrane-binding domain within the amino-terminal region of human immunodeficiency virus type 1 Gag protein which interacts with acidic phospholipids. *J. Virol.* 68:2556–2569.
67. Ziemiecki, A., H. Garoff, and K. Simons. 1980. Formation of the Semliki Forest virus membrane glycoprotein complexes in the infected cell. *J. Gen. Virol.* 50:111–123.